Available online at www.sciencedirect.com
ScienceDirect
Journal of Power Sources 177 (2008) 131–136
JOURNAL OF POWER SOURCES
www.elsevier.com/locate/jpowsour

Short communication

New electroplated aluminum bipolar plate for PEM fuel cell

Sanaa A. Abo El-Enin [a,*], Omar E. Abdel-Salam [b], Hammam El-Abd [a], Ashraf M. Amin [a]

[a] *Chemical Engineering Department, National Research Center, Cairo, Egypt*
[b] *Chemical Engineering Department, Cairo University, Cairo, Egypt*

Received 7 December 2006; received in revised form 1 October 2007; accepted 8 November 2007
Available online 22 November 2007

Abstract

Further improvement in the performance of the polymer electrolyte membrane fuel cells as a power source for automotive applications may be achieved by the use of a new material in the manufacture of the bipolar plate. Several nickel alloys were applied on the aluminum substrate, the use of aluminum as a bipolar plate instead of graphite is to reduce the bipolar plate cost and weight and the ease of machining. The electroplated nickel alloys on aluminum substrate produced a new metallic bipolar plate for PEM fuel cell with a higher efficiency and longer lifetime than the graphite bipolar plate due to its higher electrical conductivity and its lower corrosion rate. Different pretreatment methods were tested; the optimum method for pretreatment consists of dipping the specimen in a 12.5% NaOH for 3 min followed by electroless zinc plating for 2 min, then the specimen is dipped quickly in the electroplating bath after rinsing with distilled water. The produced electroplate was tested with different measurement techniques, chosen based on the requirement for a PEM fuel cell bipolar plate, including X-ray diffraction, EDAX, SEM, corrosion resistance, thickness measurement, microhardness, and electrical conductivity.

Keywords: Electroplating; Bipolar plate; PEM; Fuel cell

1. Introduction

Fuel cells are suited for applications such as automobile where quick start up is required, the core of PEM fuel cell consists of two electrodes, the anode, and the cathode separated by a polymer membrane electrolyte. The bipolar plates are the backbone of the cell that sandwich the core, provide a conduit for the flow of hydrogen and oxygen, and carry the current from the electrodes to the load circuit and vice versa.

In the design of a proton exchange membrane fuel cell, the bipolar plate remains a major cost item that still requires improvement in materials, engineering design and fabrication method. In the last decade, different research activities to manufacture alternatively bipolar plates instead of graphite plate to reduce cost and total weight of the stack is conducted. Both of ceramic and composite materials were used [1,2]; in addition, the use of coated and uncoated metals has received attention recently due to the simplicity of stamping a flow field into the metal [3]. The thin nature of the metal substrate allows for a smaller stack design with reduced weight. Inexpensive metals and alloys such as stainless steel and aluminum could easily be processed into bipolar plates [4,5]. Titanium has been suggested as an alternative for the polymer electrolyte membrane fuel cell bipolar plate material, but it is better suited for aerospace applications rather than low-cost automotive use [6].

2. Experimental work

All chemicals used throughout this work were of Analar grade and distilled water was used for preparing solutions; all solutions were freshly prepared just before application. Several nickel alloys, used as a coating layer for aluminum, are known as heat stable alloys and highly corrosion resistant. The test specimens used throughout our research were aluminum foil of alloy 1050 (thickness 0.46 mm) in a rectangular form each of dimensions 4 cm × 2.5 cm, the chemical analysis of this alloy is shown in Table 1. Each specimen was provided with a small hole for hanging in the plating cell. Each sample specimen was subjected to mechanical polishing followed by suitable pretreatment method.

The pretreatment of Al-substrate [7] is outlined in the following steps:

* Corresponding author.
E-mail address: ashmukhtar@yahoo.com (S.A.A. El-Enin).

0378-7753/$ – see front matter © 2007 Elsevier B.V. All rights reserved.
doi:10.1016/j.jpowsour.2007.11.042

Table 1
Chemical analysis of the aluminum alloy 1050

Component	Percentage (%)
Al	99.73
Fe	0.199
Si	0.049
Cr	0.001
Ti	0.016
Zn	0.001
Be	0.002
B	0.002

- Dipping in 12.5% NaOH for 3 min
- Rinsing with distilled water
- Dipping in zincating solution, which contains (10 ZnO, 100 g l^{-1} NaOH) at room temperature
- Rinsing with distilled water
- Dipping in a plating bath.

The zincating step was applied with a different time intervals of 1–3 min. The electroplating baths used in this study are given in Table 2.

3. Test techniques and measurements

The measurement techniques applied to the matrix of substrate and electroplate to evaluate the characteristics and the performance of the alloy deposits depend on the requirement of the bipolar plate. (Ni–Mo–Fe–Cr) alloy was subjected to all test techniques and measurements as produced from the plating bath and after being subjected to the annealing at 400 °C for 1 h.

The first test is the EDAX and surface morphology; the scanning electron microscope SEM photographs were recorded using SEM model Phillips XL 30 attached with EDAX unit with accelerating voltage 30 kV, magnification up to 400,000× and resolution for w (3.5 nm) can be achieved. The tested samples were pre-coated with carbon.

The X-ray diffraction technique is used to define the crystalline structure and the crystalline phases in each sample for both plated alloy and substrate. This test was done using THE BRUKER axs D8 ADVANCE model with Cu Kα radiation and nickel filter. It was adopted at 40 kV and 40 mA current at room temperature, the scanning rate was 1° min^{-1}. The electrical conductivity of the new bipolar plate is measured using OMEGA CL8400 MICRO-OHMMETER at room temperature. A "coating thickness gauges minitest" type 1003 is used to measure the coating thickness.

The hardness of the plated deposit with a thickness larger than 10 μ was measured on "Vickers" diamond microhardness tester type "Shimadzu Siesa Kusha", using a diamond pyramid dentor under a load of 50 g.

The corrosion behavior of the as-deposited Ni-alloys was tested in 10^{-4} M H_2SO_4 and 10^{-4} M HF solution, potentiodynamically using potentioscan model PGSTAT 30; graphite was used as a counter electrode and saturated calomel electrode (S.C.E) was used as the reference electrode. The electrolytic cell was made of Pyrex containing the working electrode which is the electroplated nickel alloys deposited on pretreated Al-substrate. Corrosion potential, E_{corr}; corrosion current, I_{corr}; the anodic and cathodic Tafel constants β_a and β_c, respectively were computed using a computer-controlled system.

4. Results and discussion

The pretreatment methods yield a relatively sound quality deposit, the zincating step was applied for 2 min through the research, since 2 min interval gave the best results. The chemical composition of the electroplated deposit obtained from each baths is given in Table 3, energy depressive X-ray analysis method (EDAX) was used to determine the chemical

Table 2
Ingredient and operating conditions of the electroplating baths

Ingredients	Alloy to be deposited			
	(Ni–Co)	(Ni–Fe–Co)	(Ni–Mo–Fe)	(Ni–Mo–Fe-Cr)
Nickel sulphate (M)	0.57	0.2	–	–
Nickel chloride (M)	0.126	–	0.063	0.084
Boric acid (M)	0.48	0.4	0.5	0.5
Cobalt sulphate (M)	0.038	0.06	–	–
Molybdenum chloride (M)	–	–	0.0146	0.0146
Ferrous ammonium sulphate (M)	–	–	0.0035	0.0035
Sodium citrate di-hydrate (M)	–	–	0.2	0.2
Ferrous sulphate (M)	–	0.06	–	–
Formaldehyde (M)	0.83	–	–	–
Formic acid (M)	0.507	–	–	–
Ammonium sulphate	0.06	–	–	–
Ammonium chloride (M)	–	0.3	0.5	0.5
Ascorbic acid (g l^{-1})	–	0.5	0.5	0.5
Chromium chloride (M)	−4 to 5	–	–	0.001
pH	60	3.5	5	5
Temperature (°C)	80	25	25	25
C.D (mA cm^{-2})	6.6	50	60	100
Potential (V)	10	5.3	4	5
Time (min)		10	10	10

Table 3
Deposit composition of the electroplated alloys

Deposited alloy	% of deposit components				
	Ni	Fe	Co	Cr	Mo
(Ni–Co) alloy	69		31		
(Ni–Co–Fe) alloy	32.03	32.4	35.57		
(Ni–Mo–Fe) alloy	88.46	2.9			8.64
(Ni–Fe–Mo–Cr) alloy	88.27	2.17		0.15	9.41

Table 4
Thickness, hardness, and electrical conductivity of the electroplated alloys

Alloy deposited	Thickness in μ	Hardness on Vickers hardness scale	Electrical conductivity (S/cm)
(Ni–Co)	10	230	0.34×10^6
(Ni–Co–Fe)	12	480	0.16×10^6
(Ni–Mo–Fe–Cr)	13	440	0.21×10^6
Annealed (Ni–Mo–Fe–Cr)	13	520	0.66×10^6
(Ni–Mo–Fe)	11	350	0.2×10^5

composition for each alloy. The results show that the electroplated alloys (Ni–Mo–Fe) and (Ni–Fe–Mo–Cr) have a high percentage of Ni. Electroplated (Ni–Fe–Mo–Cr) alloy is very compatible to haste alloy (B) [8], which is known as corrosion resistant alloy in acidic media such as that of PEM fuel cell.

Coating thickness is an important factor for the bipolar plate service life; the thicker the coating the longer is the life of the new bipolar plate. The thickness of electroplated alloys on Al-substrate is shown in Table 4; results show that the electroplated alloy (Ni–Fe–Mo–Cr) is the most promising for a PEM bipolar plate.

The X-ray diffraction analysis is used to identify different phases present in the as-plated and annealed electroplated nickel alloys on zincated Al-substrate from different electroplating baths under various conditions. The X-ray diffraction pattern of the as-plated electrodeposit (Ni–Co) alloy (Fig. 1) shows that the interaction between deposited nickel, cobalt and Al-substrate.

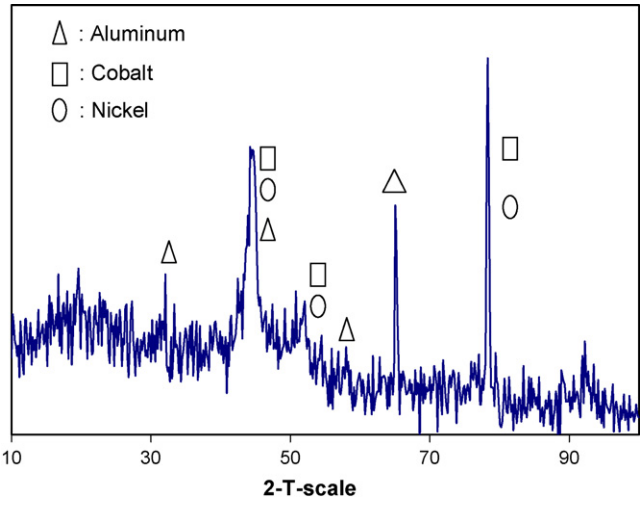

Fig. 1. X-ray diffraction for alloy (Ni–Co).

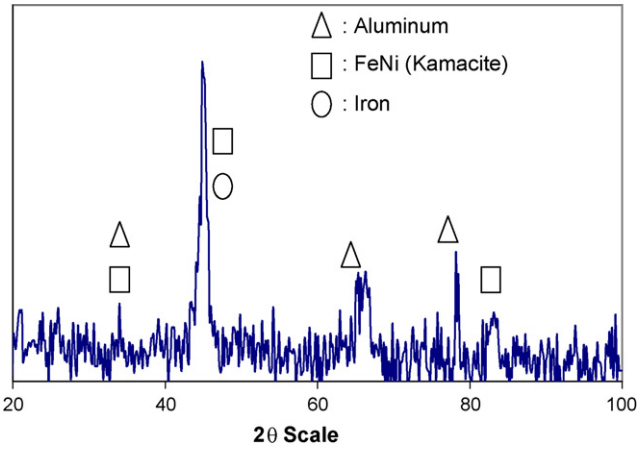

Fig. 2. X-ray diffraction for alloy (Ni–Co–Fe).

The as-plated (Ni–Co–Fe) X-ray diffraction shown in Fig. 2 has sharp peaks of Al-substrate and broad peaks of both Al-substrate and kamacite of (Fe–Ni).

In Fig. 3, X-ray diffraction pattern of the as-plated (Ni–Mo–Fe) electroplating deposit has sharp peaks containing a body-centered cubic (bcc) iron, a face-centered cubic (fcc) molybdenum, Al-substrate, and a face centered cubic molybdenum/nickel (MoNi) alloy; also, zinc appears in the hexagonal crystals form. Such as-plated deposit (Ni–Mo–Fe) alloy can be described as amorphous structure. Fig. 4, of the as-plated (Ni–Mo–Fe–Cr) alloy X-ray diffraction pattern, shows sharp peaks of Al-substrate with a cubic face centered crystals with a weak crystallinity of metallic compound of nickel chromium iron (NiCrFe), iron nickel (FeNi), and nickel with cubic face centered crystals.

The X-ray diffraction pattern of the electroplated (Ni–Mo–Fe–Cr) alloy after heat treatment at 400 °C for 1 h is shown in Fig. 5, it is clear that Al-substrate disappears and a new crystalline form of awaruite (Ni_3Fe) is formed. The percentage of nickel chromium iron (NiCrFe) increases while nickel iron alloy disappears and weak crystallinity of molybdenum and aluminum is obtained.

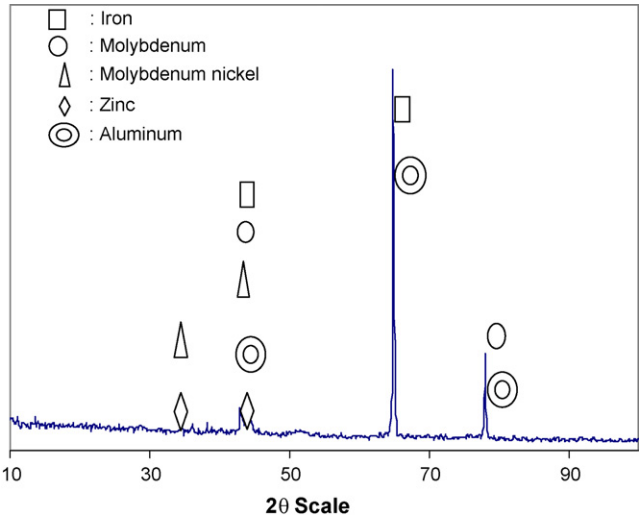

Fig. 3. X-ray diffraction for alloy (Ni–Mo–Fe).

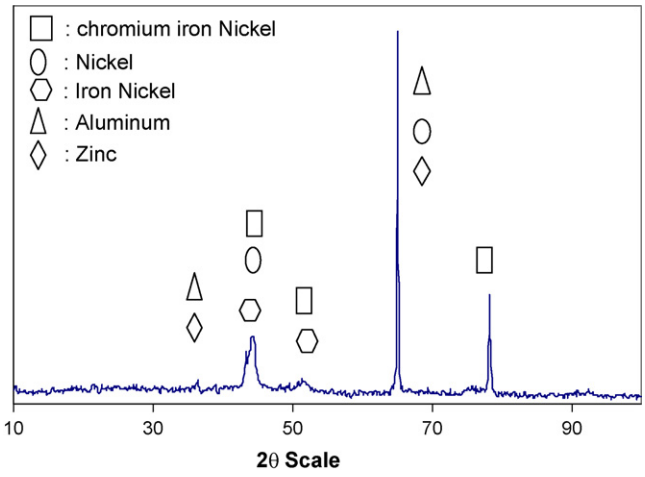

Fig. 4. X-ray diffraction for alloy (Ni–Mo–Fe–Cr).

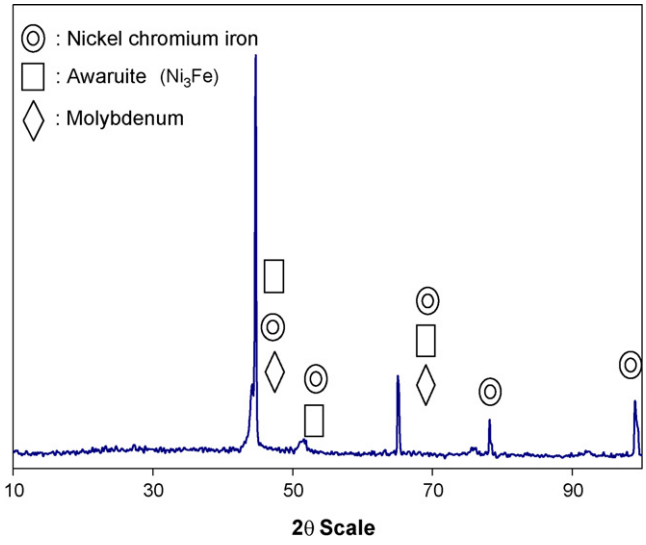

Fig. 5. X-ray diffraction for annealed alloy (Ni–Mo–Fe–Cr).

Microscopic examination of (Ni–Co) as-plated alloy shows uniform non-porous layers and coarse grains as shown in Fig. 6. The SEM of electroplated (Ni–Co–Fe) alloy, Fig. 7, shows the columnar structure of a non-porous small grain size and others of larger grain size. Fig. 8, of the as-plated (Ni–Mo–Fe) alloy of SEM revealed that, there is a dense layer with different grain size containing numerous pores between them. Figs. 9 and 10 illustrates the effect of heat treatment on the SEM of electroplated (Ni–Mo–Fe–Cr) alloy, results shows that the heat treatment at 400 °C for 1 h increases the uniformity and leveling of the deposit with a significant change in the grain size

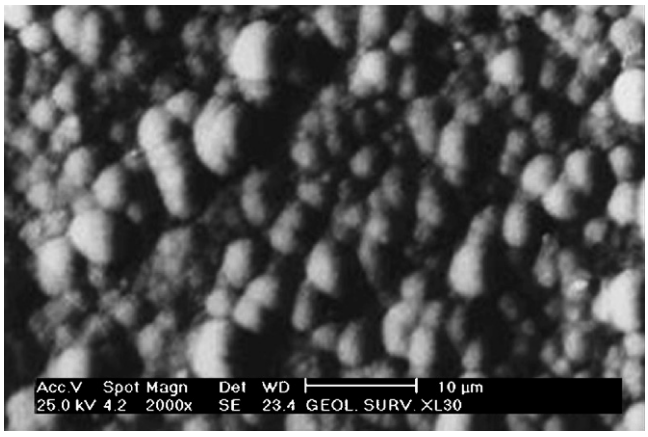

Fig. 7. (Ni–Co–Fe) alloy scan.

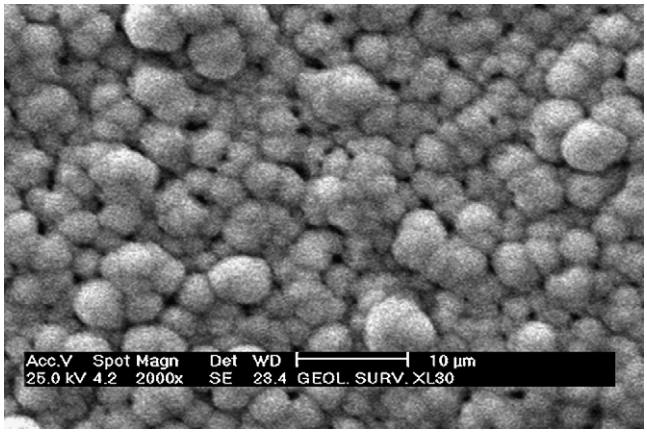

Fig. 8. (Ni–Mo–Fe) alloy scan.

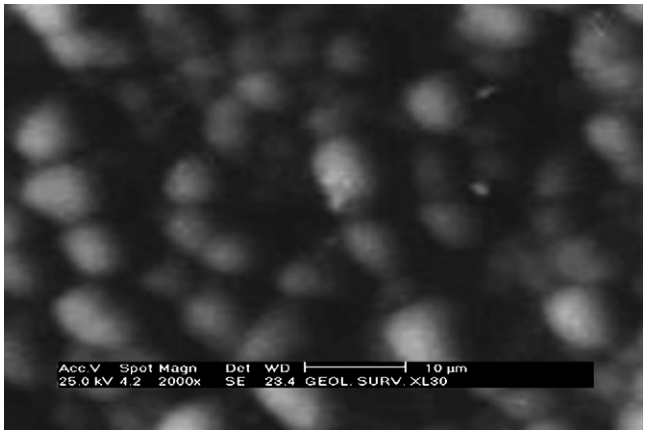

Fig. 6. (Ni–Co) alloy scan.

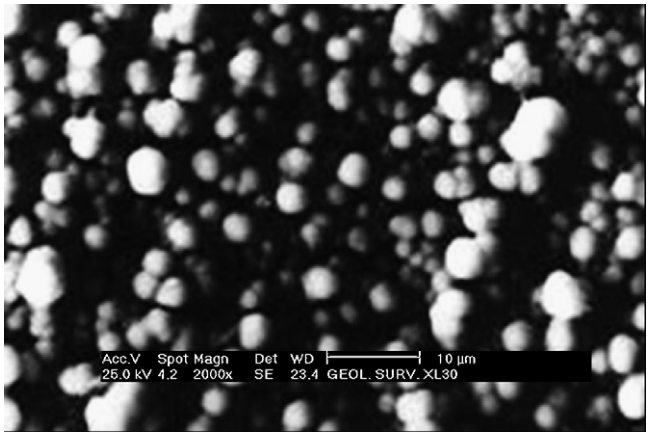

Fig. 9. (Ni–Fe–Mo–Cr) alloy scan.

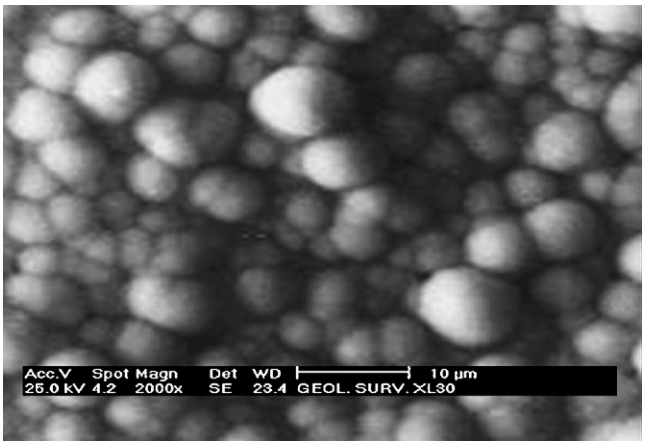

Fig. 10. Annealed (Ni–Fe–Mo–Cr) alloy scan.

and boundaries with disappearance of pores in the deposited alloy.

The microhardness test results are shown in table [4], the result shows that electroplated (Ni–Fe–Mo–Cr) is the best for PEM fuel cell application especially after annealing. This is attributed to the change in their structure, which becomes more crystalline and contains finer grains. There is a dependency of the microhardness of the deposit on their grain size; any factors, which produce small grain size, will increase the microhardness simultaneously. For fine grains, the grain boundaries hinder the slip along which deformation of the crystal would normally occurs [9]. The energy efficiency of a fuel cell system increases with increasing the electrical conductivity of the as-plated bipolar plate material. As shown in Table 4, the data of electrical conductivity illustrate that the electroplated and annealed (Ni–Fe–Mo–Cr) alloy is the most promising coating for a PEM bipolar plate.

In a H_2-air PEM fuel cell environment, the bipolar plate is in contact with a highly acidic solution (pH 3.5). Hence, metal contact elements (including bipolar plate) are subjected to anodic dissolution at the cathode, and hydrogen embitterment at the anode; so, the corrosion resistance of the electroplated nickel alloys on zincating Al-substrate was evaluated by Tafel and linear polarization methods to choice the most promising electroplated alloy to be used as a new bipolar plate in PEM fuel cell instead of graphite. The electrochemical behavior of the electroplated alloys was determined in an electrolyte containing 10^{-4} M H_2SO_4 and 2 ppm HF at 90 °C to simulate the PEM fuel cell environment using the potentiodynamic techniques [3,10]. Figs. 11–15 show the potentiodynamic polarization curves for the deposited alloys (Ni–Co), (Ni–Co–Fe), and (Ni–Mo–Fe) and the potentiodynamic polarization curve for the deposited alloy (Ni–Mo–Fe–Cr) before and after heat treatment. The electrochemical data were computed as shown in Table 5. The results in Table 5 show that (Ni–Co) alloy is the most promising one with corrosion rate of about 2 µ year^{-1} in the electrodeposited (Ni–Co–Fe) alloy, the presence of iron with the decrease of Ni % increases the corrosion rate than that of (Co–Ni). While, corrosion resistance of (Ni–Mo–Fe) alloy in such environment is very low.

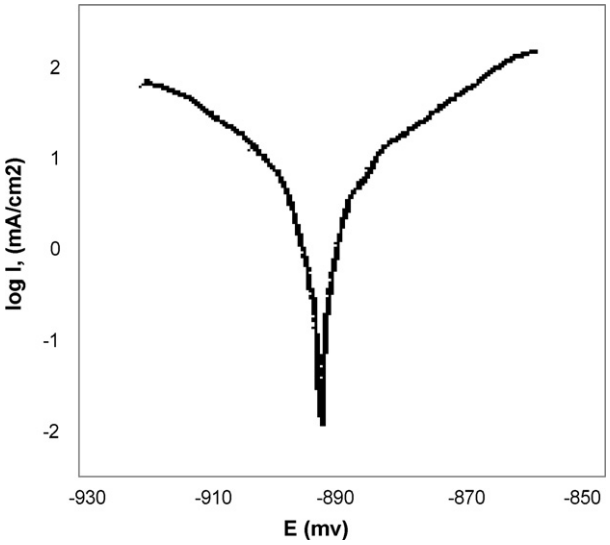

Fig. 11. Polarization curve for (Ni–Co) deposit.

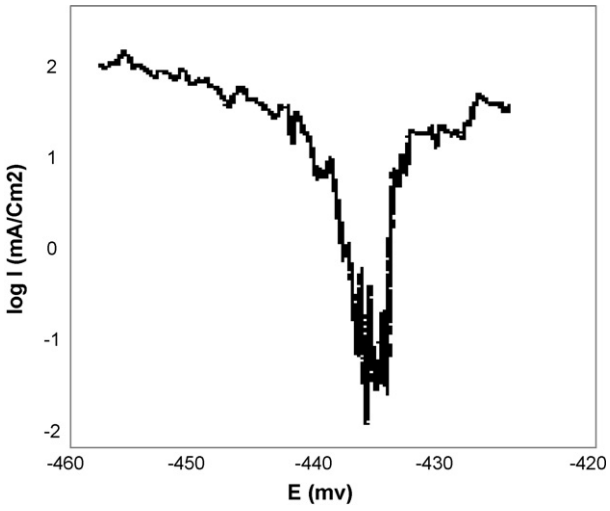

Fig. 12. Polarization curve for (Ni–Co–Fe) deposit.

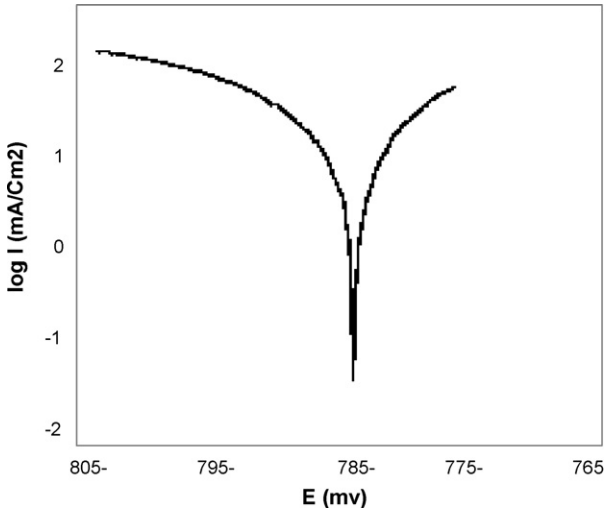

Fig. 13. Polarization curve for (Ni–Mo–Fe) deposit.

Table 5
The electrochemical data obtained from electrodeposited alloys

	Deposited alloy		Deposit composition (%)			Corrosion potential, E_{corr} (mV S.C.E^{-1})	Corrosion current, I_{corr} (μA cm^{-2})	Corrosion rate (μ year^{-1})	Polarization potential, R_p (Ω)
	Ni	Co	Fe	Cr	Mo				
(Ni–Co)	69	31				−891	0.288	2.036	5.064×10^{-3}
(Ni–Co–Fe)	32.03	35.57	32.4			−446	0.882	6.234	63.54×10^{-3}
(Ni–Mo–Fe)	88.46		2.9		8.64	−786	12.31	87	0.552×10^{-3}
(Ni–Mo–Fe–Cr)	88.27		2.17	0.15	9.41	−793	1.782	12.59	1.33×10^{-3}
Annealed (Ni–Mo–Fe–Cr)	88.27		2.17	0.15	9.41	−623	0.398	2.816	4.551×10^{-3}

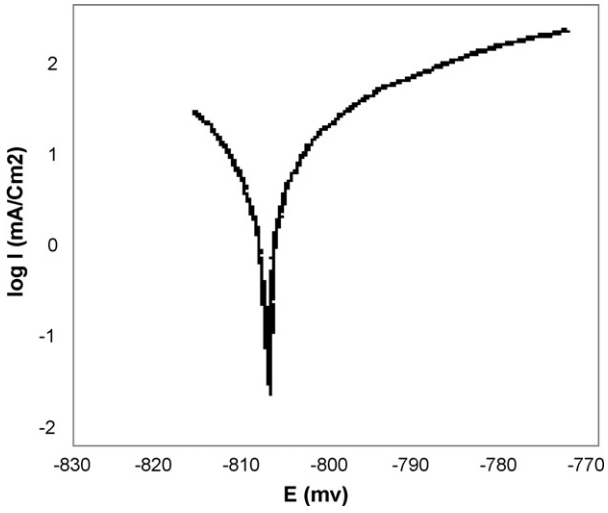

Fig. 14. Polarization curve for (Ni–Mo–Fe–Cr) deposit.

The corrosion rate of annealed (Ni–Mo–Fe–Cr) alloy at 400 °C for 1 h is smaller than that of the as-plated alloy without annealing. The corrosion rate of annealed (Ni–Mo–Fe–Cr) alloy is 2.8 μm year^{-1}, which is less than graphite corrosion rate under the same condition (15 μ year^{-1} [11]). A significant decrease in the corrosion rate of the (Ni–Co) deposit may be attributed to the formulation of microcrystalline CoNi structure as shown in the X-ray diffraction results [12].

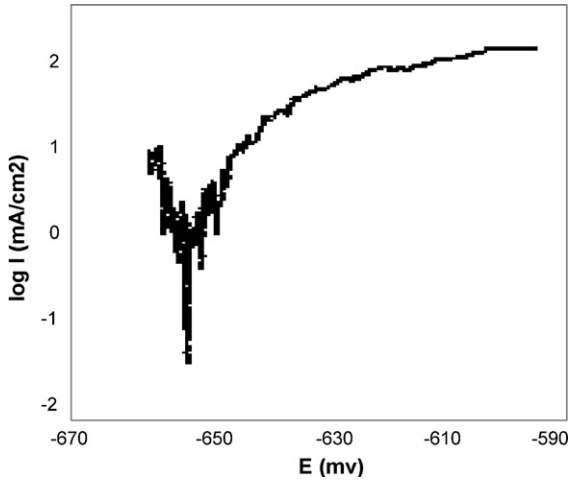

Fig. 15. Polarization curve for annealed (Ni–Mo–Fe–Cr) deposit.

5. Conclusion

The aluminum coated with (Ni–Mo–Fe–Cr) which is further annealed at 400 °C for 1 h is recommended to be used as a new bipolar plate for PEM fuel cell instead of graphite because it has several advantages compared to other electroplated alloys:

(1) High corrosion resistant in the acidic medium.
(2) Deep thickness.
(3) High-electrical conductivity.
(4) High-microhardness.
(5) Cheap ingredients, since Mo, Cr, and Ni are very cheap compared to Co.

Further work: testing of the new bipolar plate in a PEM fuel cell.

References

[1] R.J. Lawrance, Low cost bipolar current collector–separator for electrochemical cells, US Patent 4,214,969 (July 29, 1980).
[2] L. Singheiser, H.H. Bolt, H. Kobs, Bipolar plate with non-metallic coating for fuel cell, German Patent 19805683 (August 19, 1999).
[3] A.S. Woodman, K.D. Jayne, E.B. Anderson, M.C. Kimble, Light weigh and corrosion resistant metal bipolar plates for PEM fuel cells, in: Proceedings of the 34th International Society of Energy Conversion Engineering Conference, 1999, pp. 517–524.
[4] T. Kaji, T. Takikawa, Aluminum separator and its manufacture for fuel cell, Japanese Patent 135325 (May 18, 2001).
[5] D.P. Davies, P.L. Adcock, M. Turpin, S.J. Rowen, Stainless steel as bipolar plate material for solid polymer fuel cells, J. Power Sources 86 (3) (2000) 237–242.
[6] D.R. Hodgson, B. May, P.L. Adcock, D.P. Davies, New light weigh bipolar plate system for PEMFC, J. Power Sources 96 (1) (2001) 233–235.
[7] G.A. Kenneth, Electroplating Engineering Handbook, chapter 4, first ed., Reinhold Publishing Corp., New York, USA, 1955, pp. 165–178.
[8] Z. Baohua, G. Lindberg, D. Simonsson, Comparison of electrochemical and surface characterization methods for investigation of corrosion of bipolar plate materials in molten carbonate fuel cell, J. Corrosion Sci. 41 (Aug. 1999) 1497–1514.
[9] R.H. Weil, J.H. Lee, I. Kim, K. Parker, Electroless nickel plating, Plat. Surf. Finish. 2 (1989) 62.
[10] R.L. Broup, N.E. anderborgh, Design and testing criteria for bipolar plate materials for PEM fuel cell applications, Mater. Res. Soc. 393 (1995) 151–155.
[11] L. Yang, M. Wen-jin, S. Swathy, H.S. Joel, D.G. Lynn, Corrosion resistant PEM fuel cell, US Patent RE37284 (July 17, 2001).
[12] S.A.A. El-Enin, O.E. Abdel-Salam, H. El-Abd, A.M. Lotfi, New electroless nickel-alloys coated aluminum bipolar plate for PEM fuel cell, J. Mater. Sci. 1 (1–2) (2005).